

General and Inorganic Chemistry

Structure and acid-basic properties of the surface of titanium oxides modified by phosphorus and aluminum and prepared by the alkoxo method

1. Structural organization of modified titanate systems

M. V. Tsodikov,^{a*} O. V. Bukhtenko,^a E. V. Slivinskii,^a L. N. Slastikhina,^a A. M. Voloshchuk,^b
V. V. Kriventsov,^c and L. E. Kitaev^d

^aA. V. Topchiev Institute of Petrochemical Synthesis, Russian Academy of Sciences,
29 Leninsky prosp., 117915 Moscow, Russian Federation.
Fax: +7 (095) 230 2224. E-mail: tsodikov@ipc.ac.ru

^bInstitute of Physical Chemistry, Russian Academy of Sciences,
31 Leninsky prosp., 117915 Moscow, Russian Federation.
Fax: 007 (095) 952 5308

^cG. K. Boreskov Institute of Catalysis, Siberian Branch of the Russian Academy of Sciences,
6 prosp. Akad. Lavrent'eva, 630090 Novosibirsk, Russian Federation.
Fax: +7 (838 32) 64 6156

^dDepartment of Chemistry, M. V. Lomonosov Moscow State University,
Leninskie Gory, 119899 Moscow, Russian Federation.
Fax: +7 (095) 932 8846

An alkoxo method for the preparation of single-phase titanium oxides modified by phosphorus and aluminum is proposed and the mechanism of oxide formation is investigated. Structural studies showed that the sizes of the anatase microcrystallite grains and mesopores in the systems are characterized by a uniform distribution. The nature of the modifying agent and the conditions of synthesis influence the interatomic distances and the dimension of c , the tetragonal unit cell constant of anatase.

Key words: alkoxo method, tetrabutoxytitanium, crystal structure, interatomic distances, adsorption isotherm, mesopores, microcrystallites.

Among publications devoted to the preparation of new heterogeneous catalysts of the acid–base type, most numerous are those studies of acidic catalytic systems representing complex metal oxides.^{1–3} Much fewer works deal with the development of basic heterogeneous catalysts.⁴

A promising line of research into the synthesis of complex metal oxide systems is related to the use of alkoxo methods and organic precursors.⁵ It was found that single-phase complex metal oxides, which are either

substitution solid solutions or microheterogeneous highly dispersed cluster compositions, are formed rather readily in syntheses based on organic derivatives of transition metals.^{6,7}

In this paper, we report structural features of titanium oxides modified with phosphorus and aluminum ions and prepared using tetra(*n*-butoxy)titanium, ethriol phosphite (4-ethyl-2,6,7-trioxa-1-phosphabicyclo[2.2.2]-octane), and the crystal hydrate $\text{AlCl}_3 \cdot 6\text{H}_2\text{O}$, which are used as precursors in alkoxo syntheses.

These precursors contain ions (P^{3+} and Al^{3+}), which exhibit acidic and basic properties when introduced into chemical compounds. This modification is aimed at endowing catalytic systems with acidic and/or basic properties.

Experimental

Modified titanium oxides (Table 1) were prepared by the alkoxo method, in which chelation of titanium alkoxide with acetylacetone was used to stabilize the sol. For this purpose, an equimolar amount of acetylacetone was added to a 1.5 M solution of titanium tetra(*n*-butoxide). After stirring with a magnetic stirrer, argon was bubbled through the solution, while solutions of modifying components were added. A 0.5 M benzene solution of ethiol phosphite (sample 3) or a 0.5 M ethanol solution of aluminum chloride (sample 4) containing specified amounts of P or Al (see Table 1) were used as modifying reagents. The resulting sols were stirred for 30 min and 80% aqueous EtOH was added in such a way that the amount of water it contained was stoichiometric with respect to titanium alkoxide. Since the induction period of gel formation was more than 1 month, the gels were isolated by evaporation of the solvents. For comparison, titanium oxide free from modifying additives was prepared by the same procedure (sample 1) and phosphorus-containing titanium oxide was prepared by a similar procedure excluding the chelation stage (sample 2). The gels were dried *in vacuo* at 90 °C; the oxides were prepared by stepwise annealing in which the temperature increased from 100 to 500 °C over a period of 7 h.

X-Ray diffraction studies were carried out on a Dron-3M diffractometer using Cu-K α -filtered radiation. The XRAYN data bank, version 1.80, was used to identify phases based on the interplanar spacings and the relative intensities of Bragg reflections. The positions of lines characterizing the tetragonal orientation of the structure ([200] and [004]) were used to calculate the unit cell constants.⁹ The samples were scanned with a rate of 0.5° (2 θ) min⁻¹. The size of the anatase microcrystallites (the region of coherent scattering) and the microdistortion value (ϵ) were determined from X-ray line broadening.^{9,10} To separate the effects of dispersion and microdistortions, the calculations were performed using two lines and the nomogram constructed beforehand, $m_1/\beta_1 = \phi(\beta_2/\beta_1)$ and $n_2/\beta_2 = \phi(\beta_2/\beta_1)$, where β_1 and β_2 are true physical line broadenings with $d = 3.52$ and 1.89 Å, respectively; m_1 and n_2 are the fractions of physical broadening caused by the dispersity of blocks and microdistortions, respectively.

The EXAFS spectra of the Ti-K edge for all samples were recorded at the EXAFS station of the Siberian Synchrotron

Radiation Center using an electron beam energy of 2 GeV and an average current of 80 mA was used as the source of radiation. The X-ray energy was monitored with a channel cut Si(111) monochromator. The harmonic attenuation was performed by using a gold mirror. The spectra were recorded in the transmission mode using two ionization chambers filled with argon. The samples were prepared as pellets with thickness varied to obtain a 0.5–0.8 step at the absorption edge. The oscillation component $\chi(k)$ was isolated using a standard procedure.^{11–13} The background was removed by extrapolating the pre-edge region onto the EXAFS region by Viktorin's polynomials. The absorption spectra were smoothed by means of cubic splines. The inflection point at the edge of the absorption spectrum was used as the initial point E_0 of the EXAFS spectrum. The radial distribution of atoms (RDA) was calculated from the spectra in $k^3\chi(k)$ by using Fourier analysis in the -4.0 – 12.0 Å⁻¹ range of wave numbers. The structural parameters, *i.e.*, interatomic distances and coordination numbers, were determined by simulating the spectra using the EXCURV92 program¹² after preliminary Fourier filtering, resorting to known X-ray diffraction data for bulk compounds.

Parameters of the porous structure were determined from nitrogen vapor absorption isotherms at 77 K. Experimental adsorption isotherms were measured using a Yravimat-4303 automated gravimetric setup (Netch, Germany) with a sensitivity of 1 µg for a sample of up to 1 g at 77 K. The specific surface area was calculated using the BET method.¹⁴ The average pore sizes (radii) were found under the assumption of a cylindrical geometry of the pores.

The morphology of oxide systems was studied by transmission electron microscopy using a Jeol 100C electron microscope for magnifications ranging from 50 000 to 240 000. Powder samples were carefully triturated in ethanol in a jasper mortar; the resulting suspension was precipitated onto a carbon support and placed on a grid for an electron-microscopy study.

Results and Discussion

According to X-ray diffraction data, all modified oxides are single-phase systems with anatase structure (see Table 1). The nature of the modifying additive influences substantially the *c* parameter of the tetragonal lattice and microdistortions related to stresses in the crystal structure.

The results of thermogravimetric analysis and ¹³C NMR study showed that nonmodified titanium oxide, which was also prepared by alkoxo synthesis followed by calcination of the gel at 500 °C, contains residual elementary carbon (1.5–1.8 % (w/w)). In this connection, the single-phase titanium oxide can be regarded as a system modified with carbon.

According to X-ray fluorescence analysis data, samples 2 and 3 contained 1.2% (w/w) phosphorus, whereas sample 4 was found to contain 2.8% (w/w) aluminum and no more than 0.32% (w/w) chlorine. This indicates that the greater part of chlorine introduced together with the initial aluminum chloride (10.7% (w/w)) was removed during evaporation of the solvent and subsequent thermal treatment of the gel.

The values of microdistortion of the anatase lattice (Fig. 1) are inversely proportional to the dimension of lattice constant *c* of the titanium oxide containing 3 mol.% modifying agents. The intercept of the plot of

Table 1. Crystal lattice parameters, crystallite sizes, and microdistortions of single-phase oxides in the anatase structure determined by X-ray diffraction

System	<i>a</i>	<i>c</i>	<i>D</i> [*]	$\epsilon \cdot 10^{-3}$ ^{**} (rel. units)
	Å			
TiO ₂ /C (1)	3.78	9.47	195	0.9
TiO ₂ /P (2)	3.77	9.35	82	3.4
TiO ₂ /P (3)	3.77	9.41	112	2.0
TiO ₂ /Al (4)	3.78	9.42	107	1.2
TiO ₂ (5) (anatase) ⁸	3.78	9.51	—	—

* Average size of microcrystallites.

** Structure microdistortions ($\Delta d/d$).

this dependence with the abscissa axis provides, according to published data,¹⁵ the lattice constant c for the single-crystal nonmodified anatase.

Taking into account the known ion radii¹⁶ for P^{5+} , P^{3+} , Al^{3+} , and C^{0} , equal to 0.35, 0.44, 0.51, and 0.77 Å, respectively, one can assume that the linear dependence shown in Fig. 1 indicates that the atoms of the modifying agents are inserted into the anatase lattice along the [010] plane; the depth of intrusion of the modifier into the structure seems to increase with decrease in the ion radius. In addition, it can be assumed that, depending on the synthesis conditions, the phosphorus atoms occur in different oxidation states and influence the lattice microdistortion. The greatest microdistortions are caused most likely by the presence of P^{3+} , whose ion radius is 0.35 Å.

The assumption that the modifier atoms are inserted into the anatase structure is confirmed by an EXAFS study of the fine structure. Figure 2 presents RDA curves for the local environment of titanium and Table 2 shows the averaged interatomic distances in the anatase lattice from the titanium side. For comparison, the same table contains the known⁸ interatomic distances for nonmodified anatase. It can be seen that the averaged Ti—O bond lengths and one Ti—Ti interatomic distance in the systems synthesized are close to those for nonmodified anatase. The significant increase (to 0.12 Å) of the second Ti—Ti interatomic distance in the samples modified by phosphorus and aluminum implies that the modifying agents are introduced most likely along the [010] plane.

Figure 3 presents the experimental adsorption isotherms of nitrogen on the surface of the titanate systems under study, while Table 2 lists the main parameters of the porous structure. It can be seen that TiO_2/C has a small adsorption pore volume and a low specific surface. The introduction of modifiers into the structure results in substantial development of the porous structure, in which mesopores predominate. The conditions of synthesis influence the specific surface and the volume of pores; the introduction of a chelating agent at the stage of synthesis of phosphorus-containing gel results in an increase in the specific surface area and the adsorption

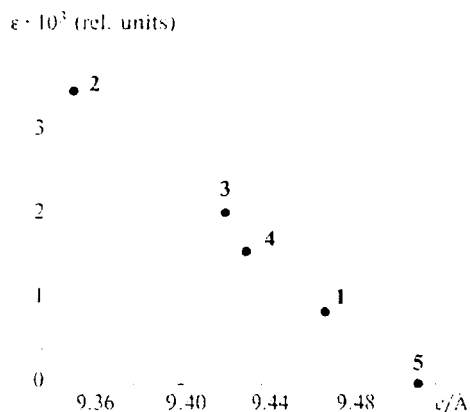


Fig. 1. Structure microdistortions (ϵ) vs. the c constant for the tetragonal unit cell of anatase for samples 1–5 (see Table 1).

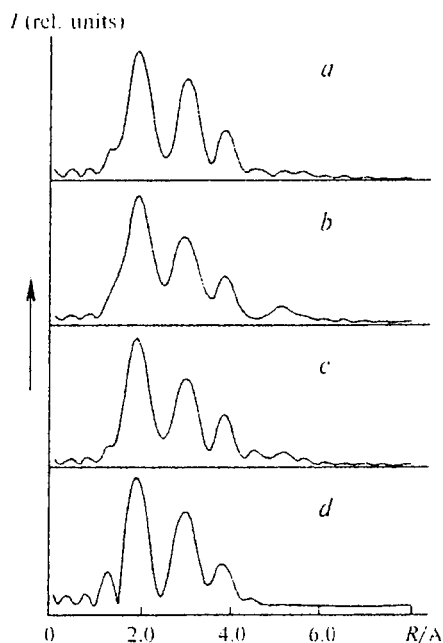


Fig. 2. Functions of radial distribution of atoms around the titanium atom for samples 2 (a), 3 (b), 4 (c), and 1 (d).

volume of pores. The isotherms of phosphorus-containing systems possessing different specific surface areas are identical in shape. The adsorption isotherm obtained for an aluminum-containing system differs markedly from those for the phosphorus-containing systems when $P/P_s > 0.45$. This result suggests that the aluminum-containing system has a wide-pore structure.

Additional information on the structure of pores can be obtained from the comparison plot¹⁷ in which the adsorption isotherm for a sample under study is compared with the isotherm measured for a nonporous sample with a similar chemical nature. Figure 4 shows the comparative plot constructed using the phosphorus-containing system 3 as the sample under investigation and the wider-pore aluminotitanate oxide 4 as the reference. The amounts of the sorbate adsorbed on the reference and test samples at equal relative pressures are laid off on the abscissa and

Table 2. Interatomic distances (R) determined by EXAFS spectroscopy and the main parameters of the porous structure (BET)

System	$R/\text{Å}$			Parameters		
	Ti—O	Ti—Ti	(Ti—Ti)'	S^*	V^{**}	r^{***}
TiO_2/C (1)	1.97	3.00	3.77	3.2	0.009	5.6
TiO_2/P (2)	1.95	3.04	3.90	34	0.031	1.82
TiO_2/P (3)	1.94	3.03	3.88	83	0.081	1.96
TiO_2/Al (4)	1.95	3.04	3.89	88	0.180	4.10
TiO_2 (5) ⁸	1.937, 1.963	3.03	3.78	—	—	—

* Specific surface area/ $\text{m}^2 \text{g}^{-1}$.

** Pore volume/ $\text{cm}^3 \text{g}^{-1}$.

*** Pore size/Å.

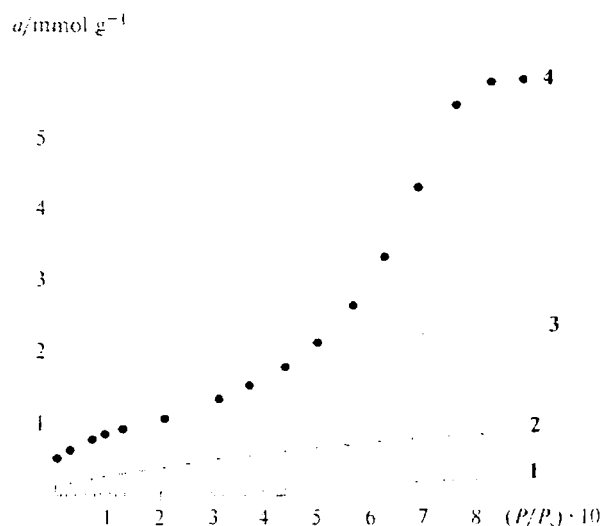


Fig. 3. Nitrogen adsorption isotherms for titanate systems 1–4; P/P_0 is the relative pressure of the adsorbate vapor.

ordinate axes, respectively. Similar plots were constructed to compare sample 4 with the other samples prepared.

The linearity of the initial section of the comparative plot indicates that, in this range of coverages, adsorption on both samples follows the same polymolecular adsorption mechanism and that the chemical nature of the surface of both samples is similar. The deviation of the comparative plot from a straight line at $P/P_0 \geq 0.45$ points to a difference between the porous structures.

As shown previously,¹⁷ the presence of a linear section on the comparison plots in the region of monolayer coverage ($P/P_0 \leq 0.45$) allows one to construct the standard adsorption isotherm over the whole range of relative pressures by the semiempirical method. The standard (reference) adsorption isotherm was constructed based on the adsorption isotherm for sample 4 in the region of monolayer coverage, while the isotherm for

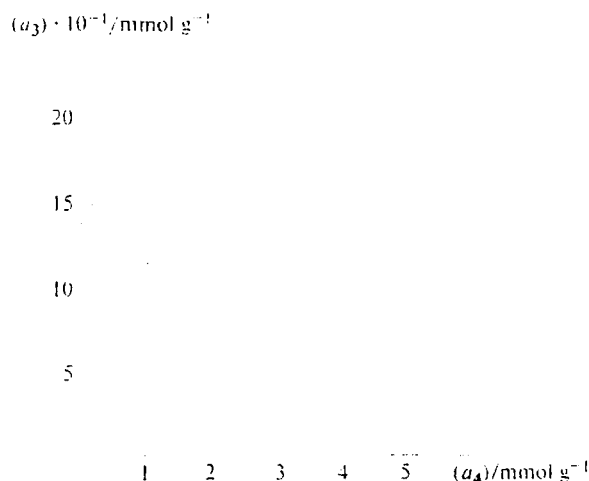


Fig. 4. Comparison plot for adsorption of nitrogen on sample 3 (TiO_2/P) and on sample 4 (TiO_2/Al).

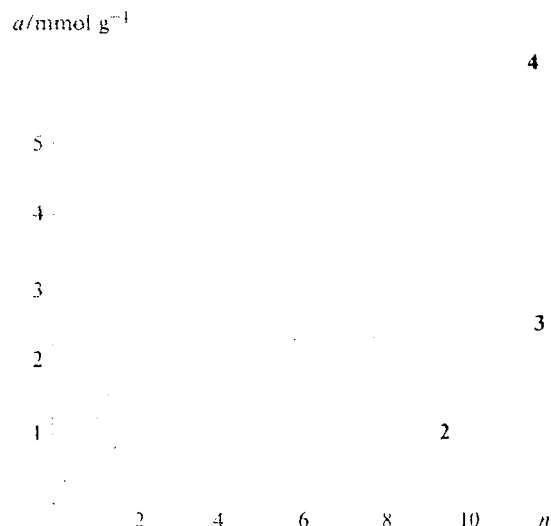


Fig. 5. Nitrogen adsorption (a) on titanate systems 2–4 vs. number of layers of adsorbed molecules (n).

polymolecular coverage was calculated using the BET equation, whose parameters were determined from the initial (monomolecular) section of the isotherm. Comparison of the adsorption on systems 2–4 with the theoretical isotherm provides the possibility of elucidating the dependence of the amount adsorbed on the number of monomolecular layers n (Fig. 5).

Analysis of the plots shown in Fig. 5 leads to several conclusions.

1. Phosphorus-containing samples 2 and 3 are characterized by equal pore sizes (x -coordinate of the break points) and different specific surface areas (proportional to the slope of the initial section of the comparison plot); hence, the pore volumes are different.

2. Phosphorus-containing sample 3 and aluminum-containing sample 4 possess similar specific surface areas but substantially different pore sizes and volumes.

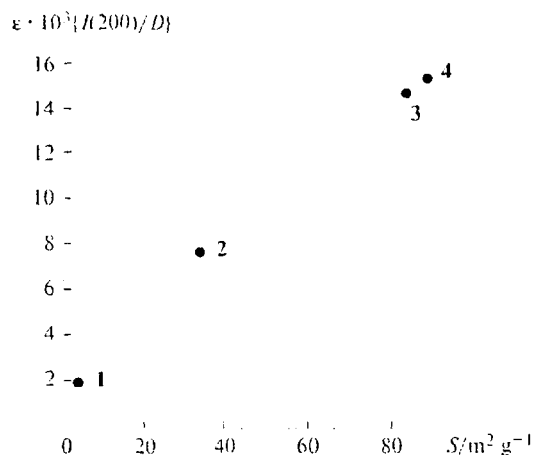


Fig. 6. Correlation of the specific surface area (S) and geometric factor of the fine structures ($\epsilon \cdot 10^3 \{I(200)/D\}$) of titanium oxides with anatase structure; I is the Miller index, D is the average size of microcrystallites.

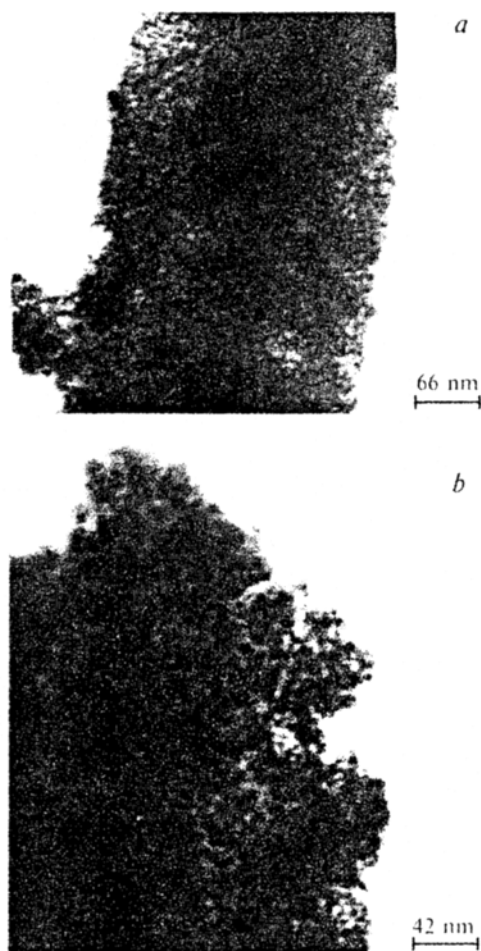


Fig. 7. Micrographs of aluminum-containing system **4** with magnifications of 150 000 (a) and 240 000 (b).

3. The uniformity of the structure of titanate oxides is indicated by correlation of the data obtained by X-ray diffraction analysis and adsorption measurements. The intensity of Bragg reflections is known¹⁸ to be proportional to the volume of the phase present in the system. In this connection, the ratio of the intensity to the broadening of the coherent scattering region with a correction applied for structure microdistortions gives a factor of fine structure adequate to the surface geometry of the sample.

4. The geometrical factor of fine structure is proportional to the specific surface areas of the oxides found from adsorption measurements (Fig. 6). This result suggests that, in addition to a uniform pore size distribution, the titanate systems are also characterized by a relatively uniform size distribution of the microcrystallites.

The data of high-resolution transmission electron microscopy confirm this assumption. It can be seen from the micrographs (Fig. 7) of the aluminium-containing system with 150 000 and 240 000 magnifications that the morphology has a uniform structure with 100–150 Å microcrystallites. The microcrystallites are separated by

relatively uniform cylindrical pores with a size of 20–30 Å. Apart from cylindrical pores, larger slit-like pores with sizes of (15–25) × (40–50) Å can also be traced on the micrograph. These pores can be formed as extended dislocations resulting from inclusion of heteroatoms into the anatase surface. The morphology of phosphorus-containing systems is also characterized by a grain structure of the microcrystallites forming the walls of cylindrical pores.

This work was supported by the Russian Foundation for Basic Research (Project No. 00-03-32407a).

References

1. A. Corma, M. I. Juan-Rajadell, J. M. Lopez-Nieto, A. Martinez, and C. Martinez, *Appl. Catal., A*, 1994, **3**, 175.
2. A. E. Kapustin, *Usp. Khim.*, 1991, **60**, 2685 [*Russ. Chem. Rev.*, 1991, **60** (Engl. Transl.)].
3. A. Corma, *Chem. Rev.*, 1995, **95**, 559.
4. V. F. Shvets, *Inzhenerno-khimicheskaya nauka dlya pere-dovykh tekhnologii* [Chemical Engineering Science for Advanced Technologies], Tr. Tret'ei Sessii, Kazan', May 26–30, 1997, Ed. V. A. Makhlin, Kazan', 1997, p. 163.
5. R. Winnerberg, M. A. Pradera, and J. A. Navio, *Langmuir*, 1997, **13**, 2373.
6. Yu. V. Maksimov, M. V. Tsodikov, O. G. Ellert, and V. V. Matveev, *J. Catalysis*, 1994, **148**, 119.
7. M. V. Tsodikov, V. Ya. Kugel, E. V. Slivinskii, G. N. Bondarenko, Yu. V. Maksimov, M. A. Alvarez, M. C. Hidalgo, and J. A. Navio, *Appl. Catal., A: General*, 2000, **193**, 237.
8. B. F. Ormout, *Struktury neorganicheskikh soedinenii* [Structure of Inorganic Compounds], Gostekhteorizdat, Moscow, 1950, p. 458 (in Russian).
9. S. S. Gorelik, L. N. Rastorguev, and Yu. A. Skakov, *Rentgenograficheskii i elektroopticheskii analiz* [X-Ray Diffraction and Electrooptical Analysis], Metallurgiya, Moscow, 1970, p. 83; p. 145.
10. J. L. Hebrard, P. Nortier, M. Pijolab, and M. Soustelle, *J. Am. Ceram. Soc.*, 1990, **73**, 79.
11. D. I. Kochubei, *EXAFS-Spektroskopiya katalizatorov* [EXAFS Spectroscopy of Catalysts], Nauka, Novosibirsk, 1992, 355 pp.
12. N. Binsted, J. V. Campbell, S. J. Gurman, and P. C. Stephenson, *SERC Daresbury Laboratory EYCUR'92 Program*, 1991.
13. M. V. Tsodikov, O. V. Bukhtenko, O. G. Ellert, V. M. Shcherbakov, and D. I. Kochubey, *Mater. Sci.*, 1995, **30**, 1087.
14. S. J. Gregg and K. S. W. Sing, *Adsorption, Surface Area, and Porosity*, Academic Press, London, 1982.
15. Joint Committee on Powder Diffraction Standards, 1995, Card No. 21-1272.
16. *Inorganic Chemistry: Principles and Elements*, Cornell University, W. A. Benjamin, Inc., New York–Amsterdam, 1965.
17. R. Sh. Mikhail, S. Brunauer, and E. E. Bodor, *J. Colloid Interface Sci.*, 1968, **26**, 45; **26**, 54.
18. A. F. Bol'shakov, N. V. Varlamov, and A. O. Dmitrienko, *Rentgenofazovyi analiz materialov elektronnoi tekhniki* [X-Ray Diffraction Analysis of Material for Electronics], Izd-vo Saratov. Univ., Saratov, 1990, 162 pp. (in Russian).

Received March 30, 2000;
in revised form June 23, 2000